Electronic Supplementary Information

Green and Sustainable Recycling of Lithium-ion Battery via Ionic Liquid-driven Cathode Reduction Method

Yin Hu[1,†], Mingchen Yang[1,†], Qingyu Dong[2], Xiuyang Zou[1], Jiangtao Yu[1], Siyu Guo[1], and Feng Yan[1,*]

[1]Jiangsu Engineering Laboratory of Novel Functional Polymeric Materials, Jiangsu Key Laboratory of Advanced Negative Carbon Technologies, Suzhou Key Laboratory of Soft Material and New Energy, College of Chemistry, Chemical Engineering and Materials Science, Soochow University, Suzhou 215123, China.

[2]CAS Center for Excellence in Nanoscience, Suzhou Institute of Nano-Tech and Nano-Bionics (SINANO), Chinese Academy of Sciences, Suzhou 215123, P.R. China.

[†]Authors with equal contributions.

* Correspondence to Feng Yan. e-mail: fyan@suda.edu.cn

Methods

Materials and Methods

1-Methylimidazole and 3-chloro-1,2-propanediol were purchased from Aladdin Reagents (Shanghai, China) Co., Ltd. Diethyl ether was purchased from Sigma-Aldrich. Polyvinylidene fluoride (PVDF) and carbon black were purchased from Shenzhen Kejing Star Technology Co., Ltd. The spent lithium batteries were supplied by the i-Lab, CAS Center for Excellence in Nanoscience, Suzhou Institute of Nano-Tech and Nano-Bionics, Chinese Academy of Sciences, Suzhou. Ultra-pure water was utilized throughout all the experiments.

Synthesis of 1-(2,3-dihydroxypropyl)-3-methylimidazolium chloride

1-(2,3-Dihydroxypropyl)-3-methylimidazolium chloride (imidazolium glycol) was synthesized according to the following steps. Simply, 1-methylimidazole (1.64 kg, 20 mol) and 3-chloro-1,2-dihydroxypropane (2.21 kg, 20 mol) were mixed and stirred at 80 ℃ for 48 hours. After that, the obtained product was further washed with ethyl acetate three times and dried under vacuum at 80 ℃.

Simulation reaction

Thermogravimetric analysis (TGA) along with mass spectra (MS) of the mixture of imidazolium glycol and lithium cobalt oxide (LCO) were carried out on STA 449 Jupiter from NETZSCH. 5 mg cathode powder (optional) and 50 μL imidazolium glycol was added into the crucible. The heating program was set to the elevated rate of 10 ℃ min^{-1} up to 120 ℃ and the temperature was kept for 2 hours in He atmosphere. The XRD were measured with a Bruker D8 diffractometer using Cu Kα radiation, and the patterns were collected in the 2θ range of 10– 60 ° with an interval time of 10 min during the leaching process at 100 ℃ under air atmosphere. The mixture of imidazolium glycol and LCO was placed in a heatable crucible.

Metal extraction using imidazolium glycol solvent

For leaching experiments, the LCO powder was added to the imidazolium glycol with an $R_{S/L}$ of 5 g L^{-1} in a closed glass bottle. The leaching efficiency of the metal ions was evaluated at different temperatures (20-120 ℃) and hours (0-72) with an oil bath. After the leaching processes, the leachate was ultracentrifugation at 10000 rpm for 5 min and the lixiviant was further filtered with a hydrophilic nylon membrane (0.45 μm pore size) to remove any undissolved residues. The obtained filtrate was used for subsequent characterization and metal ion recovery. The leaching efficiency (η) of different metals was calculated by the equation S1 below:

$$\eta = \frac{CV}{M_x} \times 100\% \qquad (S1)$$

where C is the final concentration of the metal (in mg L^{-1}), V is the volume of the initial leaching solution (in L) and M_x is the mass of the initial amount of x (Li or Co, for example) in the active material (in mg).

Metal recovery. The dissolved Co ion was collected by precipitation in an oxalic acid-rich solution. The mixed solution was stirred at 50 ℃ with a pH of 3. The precipitated pink powder CoC_2O_4 $2H_2O$ was washed with deionized water and dried at 120 ℃ under vacuum overnight. The CoC_2O_4 $2H_2O$ was further calcined at 500 ℃ for 6 hours to produce Co_3O_4. For the recovery of $LiNi_{0.6}Co_{0.2}Mn_{0.2}O_2$ (NCM622), the dissolved Ni, Co, and Mn ion in the leaching solution was collected by the oxalic acid co-precipitation process. Firstly, the concentrations of the transition ion were investigated by OCP-IES, and the molar ratio of the Ni, Co, and Mn ions in the leaching solution was altered to 1:1:1 by adding $NiCl_2$, $CoCl_2$, or $MnCl_2$ as required. Then, the solution was dropped into an oxalic acid solution. The pH of the reaction solution was controlled at 1.98 and aged for 24 hours. The precipitation was washed with ethanol and dried at 60 ℃ for 5 hours to obtain the $Ni_{1/3}Co_{1/3}Mn_{1/3}C_2O_4 \cdot 2H_2O$. The $(Ni_{1/3}Co_{1/3}Mn_{1/3})_3O_4$

precursor was obtained by the calcination of $Ni_{1/3}Co_{1/3}Mn_{1/3}C_2O_4 \cdot 2H_2O$ at a temperature of 500

℃ for 5 hours with 10 ℃ min^{-1}.

The purity (p) was defined as:

$$p=\frac{(m_{Ni}+m_{Co}+m_{Mn})/(w_{Ni}+w_{Co}+w_{Mn})}{m_{total}} \times 100\% \qquad (S2)$$

where m_{Ni}, m_{Co}, m_{Mn} is the mass of Ni, Co, Mn in the solution (mg), which were obtained based

on the data measured by ICP-OES. w_{Ni}, w_{Co}, and w_{Mn} represent the mass fraction of Ni, Co, Mn

in $Ni_{1/3}Co_{1/3}Mn_{1/3}C_2O_4 \cdot 2H_2O$ and $(Ni_{1/3}Co_{1/3}Mn_{1/3})_3O_4$. m_{total} is the mass of powder used for

OCP-IES (0.1 g), which was obtained from analytical balance.

ICP-OES. The metal ions concentrations in the imidazolium glycol filtrates were investigated

using a PerkinElmer Optima 5110 ICP-OES system. The imidazolium glycol filtrates were

diluted with 8% aqueous solution of hydrochloric acid, and at least 5 ICP standard solutions

were used to generate calibration curves, with correlation coefficients greater than 0.999. The

wavelengths were used in the axial mode: cobalt (238.892 nm), nickel (231.604 nm) manganese

(257.610 nm), and lithium (670.783 nm). The concentrations presented here are the average of

at least three replicates, and the error bars show the observed standard deviation between the

repetitions.

Ultraviolet-visible spectrometry and FTIR spectrometry. Inside a UV Lambda 750S

UV/vis/NIR spectrometer, the leachate was diluted with DMSO to an appropriate concentration

for ultraviolet (UV) analysis, and the diluted samples were inserted into a 4 mL transparent

quartz cuvette. The leachate with different temperatures and times of LCO and NCM were

measured in the range of 800 to 250 nm. The FTIR spectrometry was recorded on a Nicolet

5200 over the range of $600-4000$ cm^{-1}

Scanning electron microscopy. The morphologies of the precipitated and recycled powder were characterized using a scanning electron microscope (SEM) (Hitachi Regulus 8230, Japan) equipped with an energy dispersive spectrometer (EDS) (OXFORD Ultim Extreme EDS, UK). The microstructure of the cathode materials was characterized by the scanning transmission electron microscopy-high angular annular dark field (STEM-HAADF)

Nuclear magnetic resonance (NMR) Spectrometry and high-performance liquid chromatography-mass spectrometry (HPLC-MS). ^{1}H NMR and ^{13}C NMR spectra of the imidazolium glycol were recorded using a Bruker Avance (400 MHz) spectrometer in C_2D_6SO. The high-performance liquid chromatography-mass spectrometry was obtained by Quadrupole-time-of-flight mass spectrometer (MicroQ-TOF).

Theoretical Calculations. Density functional theory (DFT) calculations with Perdew-Burke-Ernzerhof functional (GGA-PBE) were employed to thoroughly study the interactions between imidazolium glycol and LCO by CASTEP program. For the geometry optimizations, the energy cutoff is set to be 489.9 eV, and the k points set is $1 \times 1 \times 1$ for both models. The max. force is smaller than 0.01 eV Å^{-1}, and the total energy difference should be less than 1×10^{-5} eV atom^{-1}. In all cases, there was no vibrational mode with the imaginary frequency verified for all the stable stationary points. All energy calculation was corrected with the zero-point energy.

We choose a 2x2x1 LCO unit cell with and without delithiation for the calculation models. The interaction energy between the imidazolium glycol and LCO was calculated according to Equation S3

$$E_{inter}=E_{total} - (E_{imidazolium\ glycol} + E_{LCO}) \qquad (S3)$$

where E_{inter} represents the interaction energy between the imidazolium glycol and LCO, E_{total} is the total energy of the imidazolium glycol-LCO system, $E_{imidazolium\ glycol}$ is the energy of the imidazolium glycol molecules, and E_{LCO} is the energy of LCO.

The Gibbs free energy difference is calculated based on Equation S4

$$\Delta G = E_{imidazolium\ glycol+LCO} - E_{imidazolium\ glycol+DLCO} \qquad (S4)$$

where $E_{imidazolium\ glycol+LCO}$ and $E_{imidazolium\ glycol+DLCO}$ represent the total energies of imidazolium glycol-LCO with and without delithiation.

Molecular Dynamics Simulation. Materials Studio package with the COMPASSII force field was performed to simulate the ion solvation structure of the leachate. The system contains [DHPMIM]$^+$, Li$^+$, Cl$^-$ and Co^{2+}. The molar ratio of the different ions was calculated from the ICP-OES. The periodic boundary conditions were applied in the X, Y and Z directions for all systems. The simulation process was subjected to 5 ns NPT simulation (time step = 1 fs, frame output for every 10000 steps, T = 298K, P = 0.0001 GPa), followed by a 2 ns NVT equilibrium simulation (time step = 1 fs, frame output for every 5000 steps, T = 298 K).
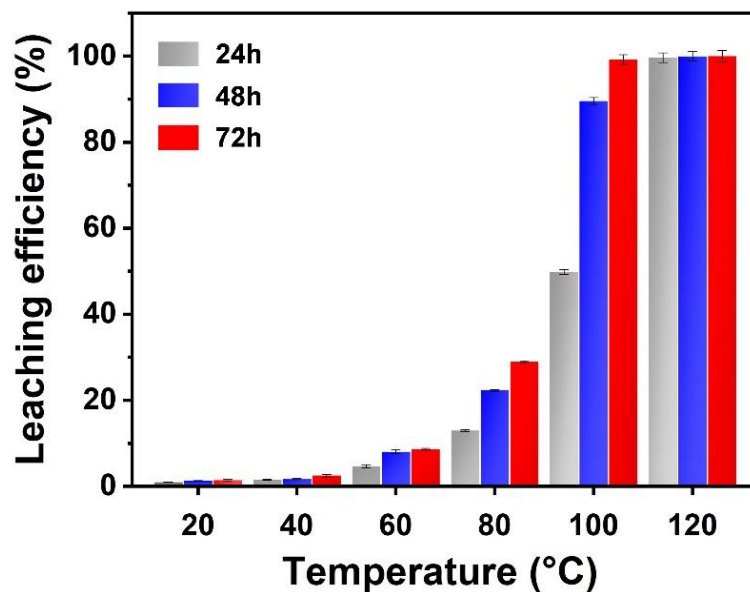
Figure S1. Relationship between cobalt leaching efficiency and temperature for different laching times illustrates the time dependence of cobalt leaching.
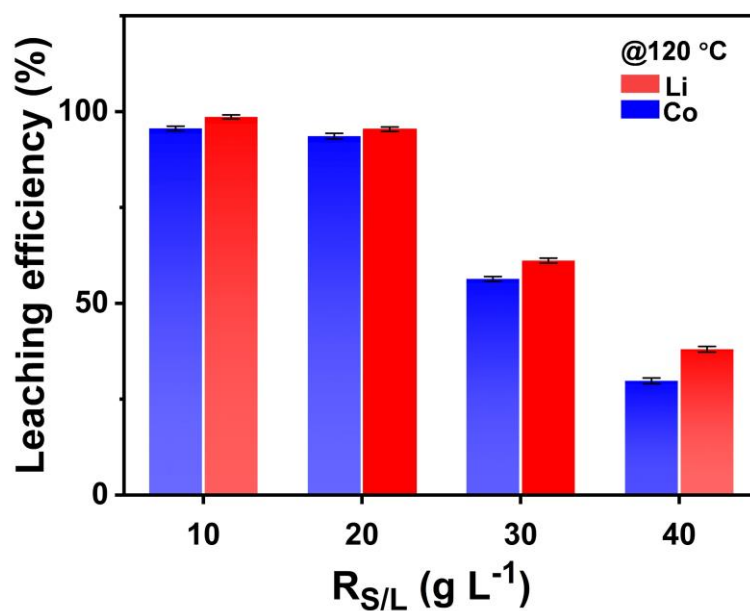

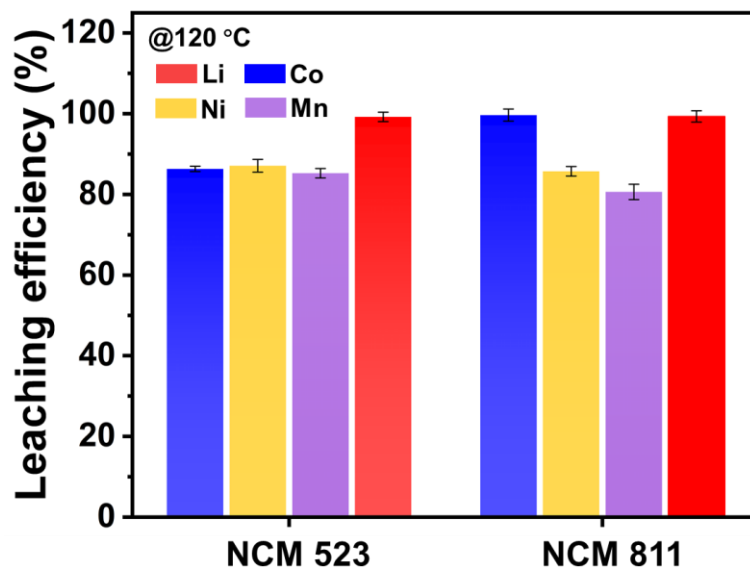**Figure S2.** Leaching efficiency of Co and Li with different $R_{S/L}$ at 120 ℃ for 20 hours.

Figure S3. Leaching efficiency of Li, Co, Ni and Mn from NCM523 and NCM811 after leaching 24 hours at 120 ℃.
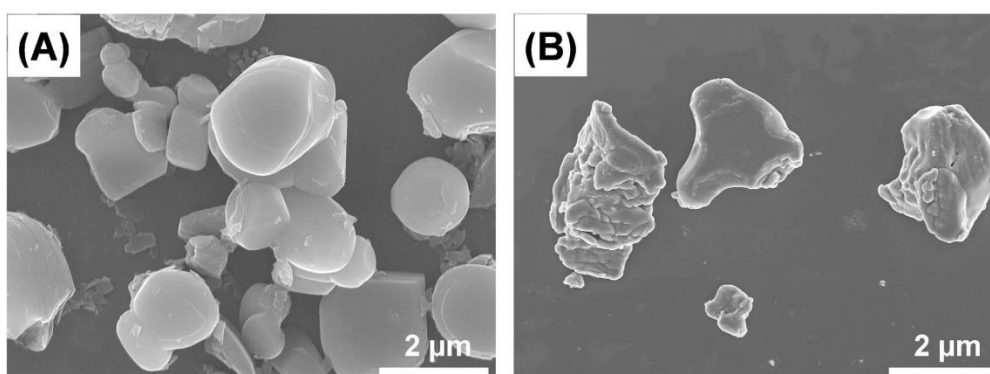

Figure S4. Scanning electron microscopy images of the LCO A) before leaching, B) after leaching at 120 °C for 4 hours.
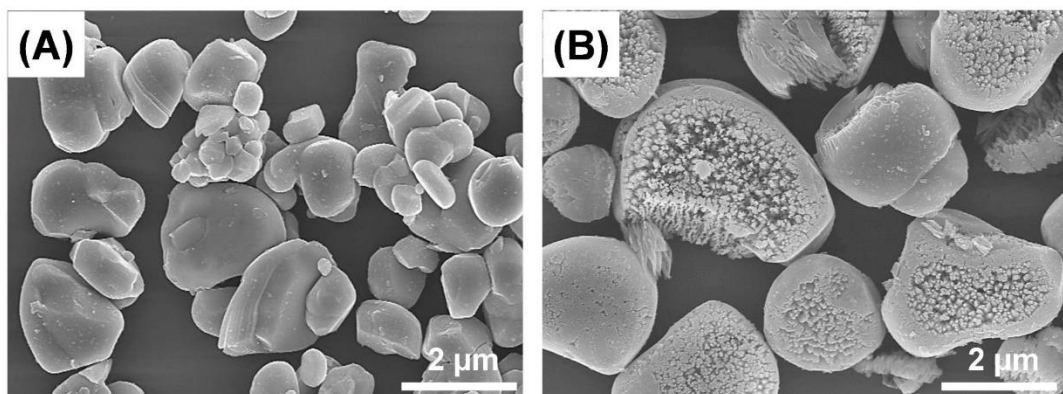
Figure S5. Scanning electron microscopy images of NCM622 A) before leaching and B) after leaching at 120 °C for 4 hours.
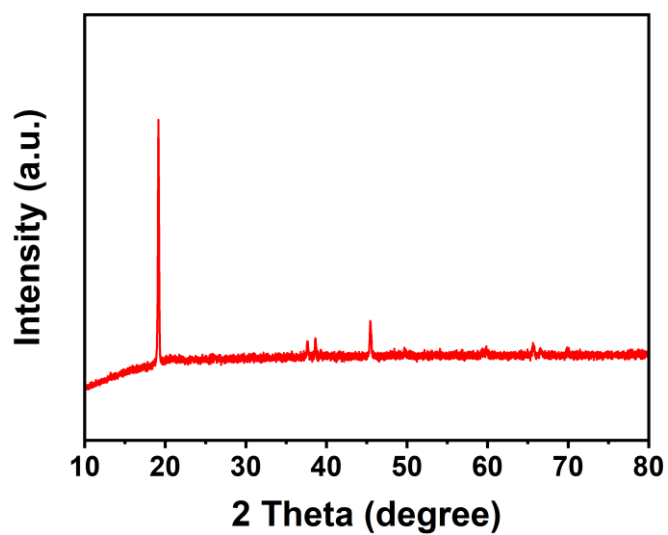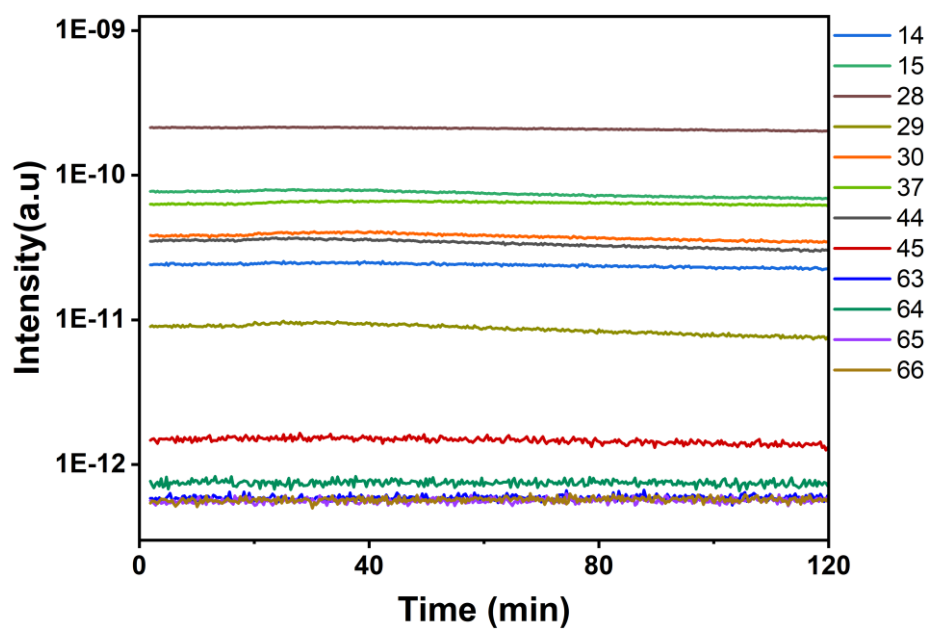

Figure S6. XRD patterns of the LCO before leaching.

Figure S7. Plot of the time-concentration curves of different mass-to-charge ratios.
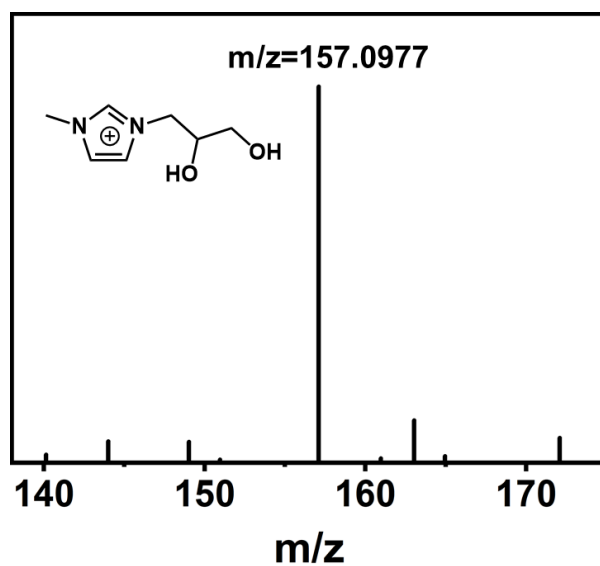
Figure S8. HPLC-MS spectra of the leachate in cation mode.
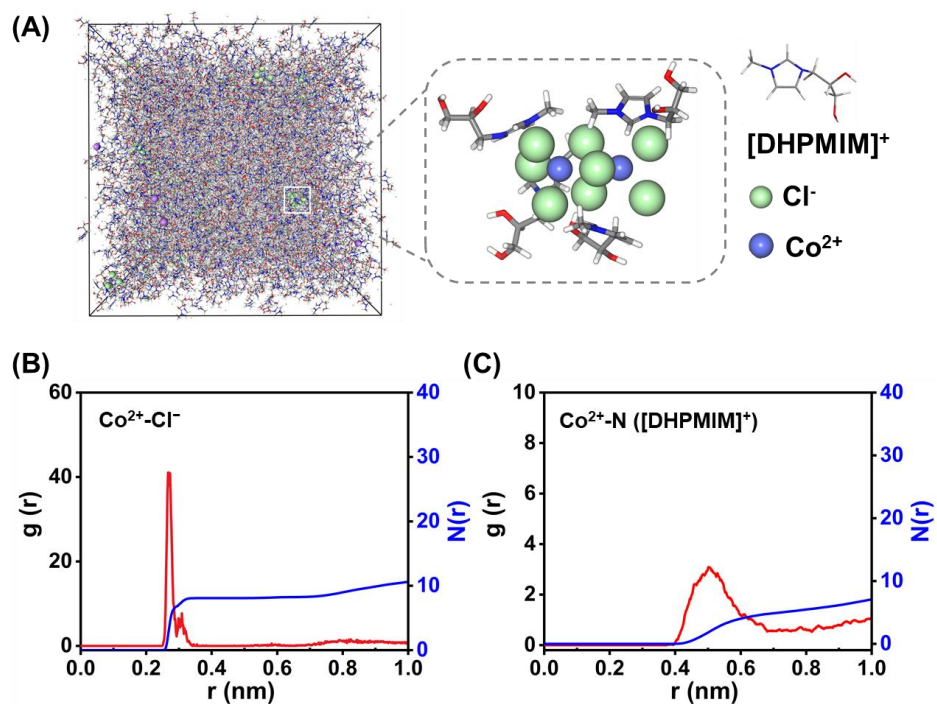
Figure S9. (A) MD simulation snapshots of leachate. The Co^{2+} presence of [DHPMIM]$_4$[CoCl$_4$]$_2$ state is displayed. (B) Radial distribution functions (RDF) of Co^{2+}-Cl^- in the leachate. (C) RDF of Co^{2+}-[DHPMIM]$^+$ in the leachate.
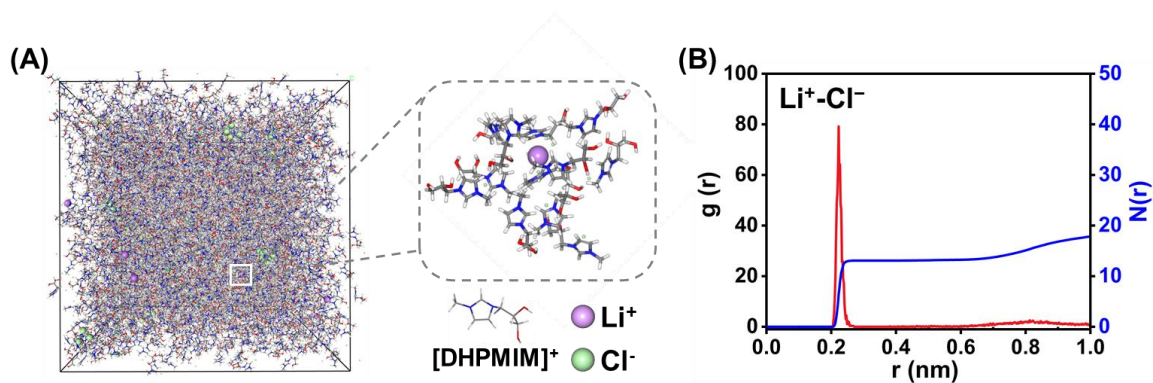
Figure S10. (A) Snapshots of the leachate. (B) Radial distribution functions (RDF) of Li^+-Cl^- in the leachate The Li presence of Li^+-Cl^- state is displayed.
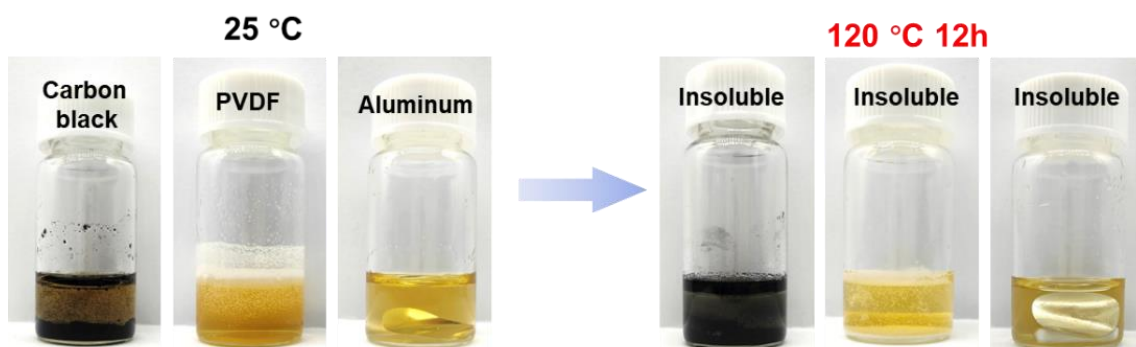
Figure S11. Leaching process of Al current collector, binder, and conductive additives in imidazolium glycol. The imidazolium glycol enables selective leaching of precious transition metals from cathode materials and releases insoluble Al current collector, binder, and conductive additives.
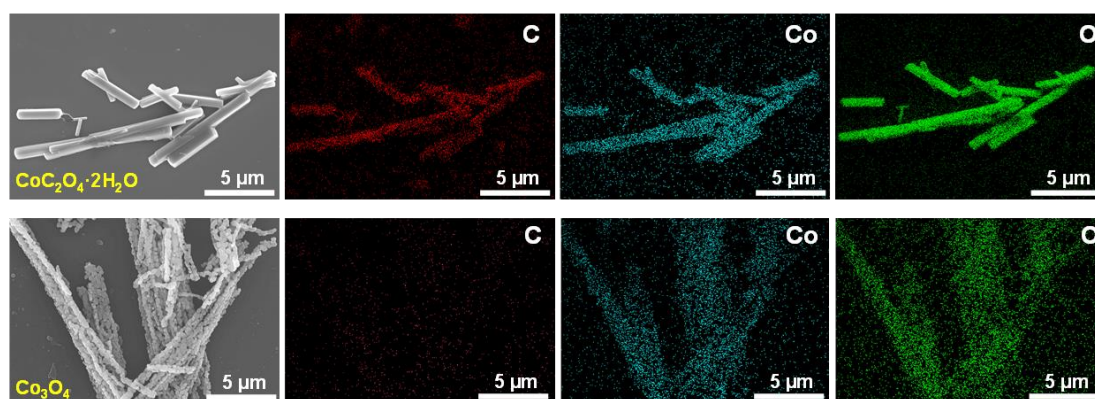
Figure S12. Scanning electron microscopy images and corresponding elemental mappings of $CoC_2O_4 \cdot 2H_2O$ and Co_3O_4.
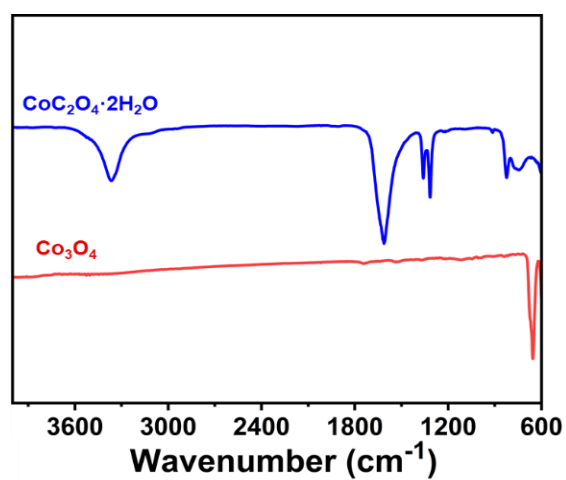
Figure S13. FTIR spectra of the recycled $CoC_2O_4 \cdot 2H_2O$ and Co_3O_4. The C-O bands at 1611 and 1362 cm^{-1} (blue curve) vanished after calcination (red curve), which demonstrates the conversion of the powder into Co_3O_4.
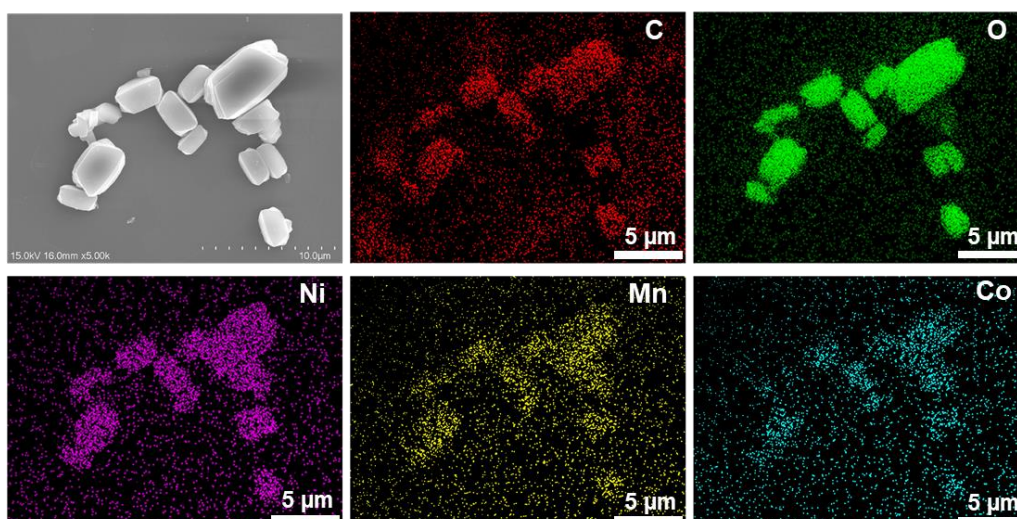
Figure S14. Morphology of the recycled $Ni_{1/3}Co_{1/3}Mn_{1/3}C_2O_4 \cdot 2H_2O$ and their corresponding EDS mapping of elemental C, O, Ni, Mn, and Co.
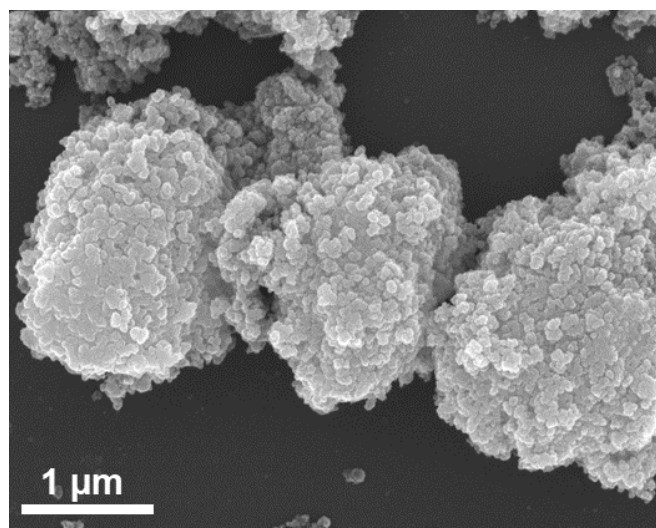
Figure S15. Scanning electron microscopy image of $(Ni_{1/3}Co_{1/3}Mn_{1/3})_3O_4$.

Figure S16. Recycling of the imidazolium glycol, the imidazolium glycol can be recovered and reused to dissolve the LCO five times with a similar color change due to its cyclability.

Table S1. Concentrations and respective leaching efficiencies of Co when leaching at the indicated temperatures for the indicated time.*

Time (h)	Temperature (˚C)	Average Co Concentration (ppm)	Standard Deviation (ppm)	Leaching Efficiency (%)
24	20	28.5	0.2	0.95
	40	47.3	0.6	1.57
	60	138.3	1.5	4.59
	80	388.3	2.5	12.90
	100	1496.6	14.7	49.71
	120	2999.5	34.1	99.63
48	20	39.9	0.2	1.33
	40	51.0	0.5	1.69
	60	240.9	1.5	8.00
	80	669.8	2.8	22.25
	100	2686.6	23.8	89.24
	120	3009.5	32.1	99.96
72	20	42.3	0.6	1.41
	40	75.3	1.1	2.50
	60	258.8	1.3	8.60
	80	869.4	3.2	28.88
	100	2976.0	36.3	98.85
	120	3010.1	39.4	99.98

*Averages and standard deviations are based on at least three replicates at each leaching temperature.

Table S2. Concentrations and respective leaching efficiencies of Co when leaching for different hours at 120 °C.*

Extracted Element	Time (h)	Average Concentration (ppm)	Standard Deviation (ppm)	Leaching Efficiency (%)
Co	4	1333.3	31.8	44.28
	8	2040.4	21.1	67.78
	12	2808.8	44.2	93.30
	16	2851.5	31.8	94.72
	20	2999.1	44.8	99.62
	24	2999.5	34.1	99.63
Li	4	161.3	15.8	45.97
	8	243.9	17.7	69.49
	12	333.7	15.1	95.06
	16	344.0	10.0	98.00
	20	351.0	25.2	100.00
	24	351.0	35.1	100.00

*Total concentrations of the Co and Li were 3010.5 and 351 ppm. Averages and standard deviations are based on at least three replicates at each leaching hour.

Table S3. Concentrations and respective leaching efficiencies of the Co, Ni, Mn and Li for NCM622 when leaching for different hours at 120 °C.*

Extracted Element	Time (h)	Average Concentration (ppm)	Standard Deviation (ppm)	Leaching Efficiency (%)
Co	4	212.0	1.3	32.50
	8	315.7	1.6	45.78
	12	371.9	2.3	54.63
	16	449.5	1.9	64.29
	20	494.7	1.8	72.35
	24	602.5	2.0	89.65
Ni	4	589.5	5.1	30.22
	8	921.5	7.6	44.70
	12	1106.6	8.1	54.38
	16	1306.8	18.8	62.51
	20	1439.5	15.6	70.40
	24	1725.2	18.9	87.43
Mn	4	185.4	2.4	30.46
	8	288.6	2.9	44.85
	12	339.1	3.6	53.40
	16	409.4	3.7	62.75
	20	450.6	3.1	70.63
	24	556.0	4.7	87.66
Li	4	130.1	3.4	39.6
	8	186.2	7.5	56.67
	12	225.6	6.2	68.67
	16	265.9	3.0	80.93
	20	280.0	6.9	85.24
	24	**327.4**	**8.7**	**99.67**

*Total concentrations of the Co, Ni, Mn, and Li were 641.5, 1918, 598.5, and 328.5 ppm, respectively. Averages and standard deviations are based on at least three replicates at each leaching hour.

Table S4. Concentrations and respective leaching efficiencies of the Co, Ni, Mn and Li for NCM523 when leaching 24 h at 120 °C.*

Extracted Element	Average Concentration (ppm)	Standard Deviation (ppm)	Leaching Efficiency (%)
Co	526.7	3.5	86.34
Ni	1324.2	20.9	87.12
Mn	729.1	8.6	85.28
Li	357.2	6.1	99.22

*Total concentrations of the Co, Ni, Mn, and Li were 610, 1520, 855, and 360 ppm, respectively. Averages and standard deviations are based on at least three replicates.

Table S5. Concentrations and respective leaching efficiencies of the Co, Ni, Mn and Li for NCM811 when leaching after 24 h at 120 °C.*

Extracted Element	Average Concentration (ppm)	Standard Deviation (ppm)	Leaching Efficiency (%)
Co	303.9	4.7	99.67
Ni	2070.3	24.6	85.73
Mn	225.8	4.3	80.64
Li	352.7	5.4	99.35

*Total concentrations of the Co, Ni, Mn, and Li were 305, 2415, 280, and 355 ppm, respectively. Averages and standard deviations are based on at least three replicates.

Table S6. Co and Li leaching efficiency for the leaching kinetics analysis.

Extracted Element	Time (min)	Leaching Efficiency (%)
Co	20	4.89
	60	10.69
	100	17.99
	240	44.28
	480	67.78
Li	20	5.62
	60	12.53
	100	18.37
	240	45.97
	480	69.49

Table S7. ICP-OES analysis of $Ni_{1/3}Co_{1/3}Mn_{1/3}C_2O_4 \cdot 2H_2O$.*

Element	Ni	Co	Mn
Mass (mg)	10.68	10.80	9.98
$n_{(Ni)}: n_{(Co)}: n_{(Mn)}$		0.99:1.00:0.99	
Purity (%)		99.33	

*Total mass of $Ni_{1/3}Co_{1/3}Mn_{1/3}C_2O_4 \cdot 2H_2O$ was 0.1 g, and the mass of Ni, Co, Mn from the ICP-OES test was 10.68, 10.80, 9.98 mg, respectively.

Table S8. ICP-OES analysis of $(Ni_{1/3}Co_{1/3}Mn_{1/3})_3O_4$.*

Element	Ni	Co	Mn
Mass (mg)	24.88	24.90	23.04
$n_{(Ni)}: n_{(Co)}: n_{(Mn)}$		1.00:1.00:0.99	
Purity (%)		99.41	

*Total mass of the $(Ni_{1/3}Co_{1/3}Mn_{1/3})_3O_4$ was 0.1 g, and the mass of Ni, Co, Mn from the ICP-OES test was 24.88, 24.90, 23.04 mg, respectively.

Table S9. Summary of LIBs recycling using different systems for metals recovery.*

	Cathode materials	Agents	Leaching efficiency	Agents Recycle	Temperature (°C)	Reference
Pyromet-allurgy	$LiCo_{1-x}Ni_xO_2$	$FeO+SiO_2+Al_2O_3$ slag	98.83% Co, 98.39% Ni, 93.57% Cu	NO	1450	S1
	NCM	Spent anode powder	82.2% Li, 97.7% Ni 99.1% Co	NO	650	S2
	$LiCoO_2$	$(NH_4)_2SO_4$	91.3% Li, 93.5% Co	NO	400	S3
Hydrometall-urgy	LCO	$1M\ HNO_3+1.7$ vol% H_2O_2	95% Li and Co	NO	75	S4
	Spent cathode	$1M\ H_2SO_4+0.075\ M$ $NaHSO_3$	93.4% Li, 66.2% Co, 96.3% Ni 50.2% Mn	NO	95	S5
	LCO	1.25M citric acid+1.0 vol% H_2O_2	100% Li, 90% Co	NO	90	S6
	LCO	1M maleic acid+1.5 vol% H_2O_2	99.58% Li, 98.77% Co	NO	70	S7
DES	LCO	ChCl–EG	94% Li, 90 %Co	Yes	220	S8
	LCO	ChCl–Urea	94.7% Li, 97.9 %Co	NO	180	S9
	LCO	ChCl–OAD	96.1% Li, 96.3% Co	Yes	120	S10
ILs	LCO	Imidazolium glycol	100% Li, 99.67% Co	Yes	120	This work
	NCM	Imidazolium glycol	99.67% Li, 89.65% Co, 87.43% Ni 87.66% Mn			

*The energy usage is estimated based on the leaching temperature, and environmental friendliness is assessed based on the environmental friendliness of the leaching agent. The Pyrometallurgy recycling process requires high-temperature calcination and acid leaching, resulting in higher energy consumption and pollution.[S11] The organic acids are environmentally friendly compared to inorganic acids, and DES and ILs do not require extra reducing agents or waste treatment which are more environmentally friendly than traditional hydrometallurgy.[S12,S13] The leaching efficiency is estimated based on the leaching efficiency of Li and Co.

References

S1   G. Ren, S. Xiao, M. Xie, B. Pan, J. Chen, F. Wang and X. Xia, *Trans. Nonferrous Met. Soc. China*, 2017, **27**, 450–456.

S2   Y. Ma, J. Tang, R. Wanaldi, X. Zhou, H. Wang, C. Zhou and J. Yang, *J. Hazard. Mater.*, 2021, **402**, 123491.

S3   J. Lin, C. Liu, H. Cao, R. Chen, Y. Yang, L. Li and Z. Sun, *Green Chem.*, 2019, **21**, 5904–5913.

S4   C. Lee and K. Rhee, *J. Power Sources*, 2002, **109**, 17–21.

S5   P. Meshram, B. Pandey and T. Mankhand, *Chem. Eng. J.*, 2015, **281**, 418–427.

S6   L. Li, J. Ge, F. Wu, R. Chen, S. Chen and B. Wu, *J. Hazard. Mater.*, 2010, **176**, 288–293.

S7   B. Liu, Q. Huang, Y. Su, L. Sun, T. Wu, G. Wang, Q. Zhang and F. Wu, *ACS Sustain. Chem. Eng.*, 2020, **8**, 7839–7850.

S8   M. Tran, M. Rodrigues, K. Kato, G. Babu and P. Ajayan, *Nat. Energy*, 2019, **4**, 339–345.

S9   S. Wang, Z. Zhang, Z. Lu and Z. Xu, *Green Chem.*, 2020, **22**, 4473–4482.

S10   Q. Lu, L. Chen, X. Li, Y. Chao, J. Sun, H. Ji and W. Zhu, *ACS Sustain. Chem. Eng.*, 2021, **9**, 13851–13861.

S11   G. Harper, R. Sommerville, E. Kendrick, L. Driscoll, P. Slater, R. Stolkin, A. Walton, P. Christensen, O. Heidrich, S. Lambert, A. Abbott, K. Ryder, L. Gaines and P. Anderson, Nature, 2019, **575**, 75–86.

S12   J. Wang, Y. Lyu, R. Zeng, S. Zhang, K. Davey, J. Mao and Z. Guo, Energy Environ. Sci., 2023, **17**, 867–884.

S13   J. Mao, C. Ye, S. Zhang, F. Xie, R. Zeng, K. Davey, Z. Guo and S. Qiao, Energy Environ. Sci., 2022, **15**, 2732–2752.